Protein adhesion on water stable atmospheric plasma deposited acrylic acid coatings

Mick Donegan and Denis P Dowling*

School of Mechanical and Materials Engineering, University College Dublin, Belfield, Dublin 4, Ireland

*Email: denis.dowling@ucd.ie

Abstract

There is considerable interest in the application of plasma polymerised acrylic acid (ppAAc) coatings due to their ability to enhance the adhesion of cells and proteins. An issue with this coating however it its stability in water and previous studies carried out using low pressure plasmas have demonstrated that high plasma powers are required to achieve water stable coatings. In this paper the use of both helium and air atmospheric plasmas are compared for the deposition of ppAAc coatings. The deposition studies were carried out on silicon wafer substrates using the PlasmaStream™ and PlasmaTreat™ plasma jet deposition systems respectively. The coatings were characterized using contact angle, FTIR, SEM, XPS, ellipsometry and optical profilometry. While both the helium and air plasmas were successful in the deposition of ppAAc coatings, the nm thick films deposited using the PlasmaTreat system exhibited significantly higher levels of water stability, probably due to a higher level of coating cross linking. Ellipsometry measurements demonstrated only a 0.2 nm reduction in the thickness of an 18 nm thick ppAAc coating, when immersed in an aqueous buffer solution for one hour. Protein attachment studies were carried out using a flow cell system, which was monitored using a spectroscopic ellipsometer. This study was carried out with Bovine Serum Albumin (BSA), Immunoglobulin G (IgG) and Fibrinogen (Fg) proteins. In all three cases increased levels of protein adhesion was observed for the ppAAc coating, compared to that obtained on the uncoated silicon wafer substrates.

Keywords: Atmospheric Plasma, Thin Film, Nano-coatings, Surface Engineering, Protein Adhesion

1.0 Introduction

Controlling protein adhesion is an important issue affecting many different fields including bio-processing, medical device implants, biosensors, and drug delivery devices [1, 2]. When the surface of a material interacts with a biological environment one of the initial interactions is through protein adhesion [3]. Amongst the factors influencing protein adsorption, are surface chemical functionality and morphology [4]. Amongst the techniques that have been investigated to modify the surfaces of polymers prior to protein adhesion studies have been micro patterning and monomer polymerisation by free radical solution, emulsion, grafting as well as plasma processes [5-9]. It has been demonstrated by a number of authors that plasma techniques enable both the surface functionality and morphology to be tailored [10, 11]. This makes it possible to create a surface which will inhibit or enhance the rate of protein adhesion onto a biomaterial surface, without changing the properties of the bulk material [12].

One surface chemistry that has received considerable attention for cell and protein adhesion has been acrylic acid. Surfaces containing this coating have been reported in applications ranging from platelet adhesion promotion [13], RGD peptide immobilisation [14], attachment of osteoblast-like [15], fibroblast [16] and keratinocyte [17] cells as well as collagen molecule grafting [18].

To-date low-pressure plasma processes have been extensively investigated for the deposition of plasma polymerised acrylic acid (ppAAc) coatings. These include: radiofrequency (13.56 MHz) parallel plate [14, 15, 19], glow discharge [16] and two-phase plasma polymerisation processes [20]. The coatings obtained using these techniques displayed similar properties such as the retention of a high degree of monomer structure and functionality. Coatings deposited at lower plasma powers were not found to exhibit good stability in water, the use of higher powers were required to yield coatings exhibiting greater stability in aqueous solutions [16]. These latter coatings were dominated by ester functionalities and were highly cross-linked.

The enhanced stability of the ppAAc coatings however was found to be associated with a reduction in COOH functionality [14]. This is due to high fractionalisation of the acrylic acid monomer.

There have been a small number of reports on the use of dielectric barrier discharge, atmospheric pressure plasmas for the deposition of ppAAc coatings [7, 21]. Here too it was reported that as plasma power is increased the percentage of carboxyl functionalities decreases. These papers do not discuss the water stability issues associated with ppAAc, however; lower power plasma deposited coatings were reported to exhibit more hydrophilic properties (water contact angles under 20º). Coatings deposited at higher plasma powers in contrast had contact angles up to water contact angles of 45° indicating a high organic content possible due to the loss of –COOH functionality.

The objective of this study is to investigate the deposition of ppAAc coatings using both a helium and air based atmospheric plasma systems. The focus of this study is to firstly compare the properties of the coatings deposited using the two atmospheric plasma jet systems and in particular to evaluate the water stability of the deposited coatings. Once a relatively water stable coating is achieved the study will investigate the effect of the ppAAC coating on the adhesion of three different types of protein in an aqueous buffer solution.

2.0 Experimental

2.1 Coating Deposition

The helium atmospheric plasma studies were carried out using the PlasmaStream™ (Dow Corning Plasma Solutions) system, which has been described previously [22, 23]. In this system

the discharge is formed using a modified PTI 100 W rf power supply, between two pin electrodes. This is a high voltage source that uses a flyback transformer, which produces a non-sinusoidal voltage waveform due to the rapid collapse of the magnetic circuit within the flyback transformer [23]. Liquid precursors are nebulised between these electrodes using a pneumatic Burgener Mira Mist nebuliser. The nebulised liquid is mixed with helium and nitrogen gasses inside a Teflon tube, 75 mm long and 15 mm in diameter, mounted over the power source. A plasma is formed inside this tube and extends out of its base, under which the substrate is placed (Figure 1). The plasma formed operates at a frequency of between 15 - 25 kHz, with maximum output voltages between 11.8 and 14.9 kV. The distance from the base of the tube to the substrate, as well as the speed at which the jet moves, is controlled by a computer numerical control (CNC) system. The air plasma deposition studies were carried out using the PlasmaTreat OpenAir^{TM} system, which has also been described previously [10, 22, 24]. This system (Figure 2) operates by forming a blown arc inside an arc cavity as ionised gas is expelled through a 5 mm (PFW10) jet nozzle. The 25 kHz plasma jet is driven by a positive uni-polar square wave pulse width modulation (PWM) transistor amplified circuit. A pneumatic liquid precursor delivery system is used to deliver the AAc through a heating coil and then directly into the plasma. The plasma is formed using dry compressed air at inlet pressures of between 100,000 and 300,000 Pascal. The system operates at airflow rates of between 37.5 and 76.61 $l.min^{-1}$.

Coatings were deposited using an acrylic acid (Sigma Aldrich 99%) precursor onto silicon wafers (450 μm thick, p-type, boron doped and polished on one side). The wafers had previously been ultrasonically cleaned in methanol, dried, then cleaned ultrasonically in acetone and re-dried.

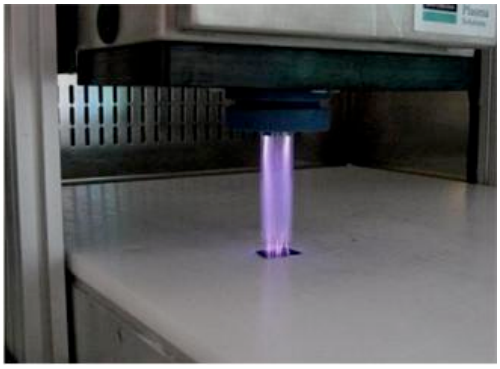

Figure 1: Helium plasma formed using the PlasmaStream™ atmospheric plasma jet system

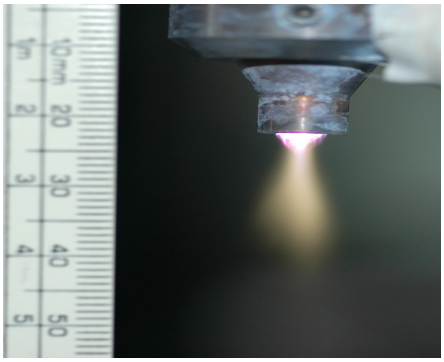

Figure 2: Air plasma formed using the PlasmaTreat OpenAir™ atmospheric plasma jet system

2.2 Coating Characterisation

A Dataphysics Instruments OCA 20 Video Based Contact Angle Device utilised the sessile drop technique to obtain water contact angles, using deionised water at room temperature. 1 μl drops were allowed to sit on the surface for 5 seconds (approx.) before contact angles were measured. Measurements were taken from three different locations on three different samples, an average of these was then calculated. These measurements were taken one week after coatings were deposited in order to minimise activation effects of the plasma on the silicon wafer substrate. Surface energies were determined using deionised water, diodomethane and ethylene glycol. The OWRK method was then employed to calculate the surface energy of the deposited coatings based on the contact angles obtained [25, 26].

A Woolam M2000 (J.A.Woolam Co. Inc., USA) variable wavelength ellipsometer was used to determine film thickness on the silicon wafer. Measurements were taken at three different points on each of the test samples. Light of known polarisation reflects off of and refracts through the coatings. This results in a change in the polarisation of the light. This change is recorded and a Cauchy model is fitted to the data to indicate film thickness [27]. Coating stability in phosphate buffer solution was also monitored dynamically using this technique.

Optical profilometry measurements were used to determine morphologies and roughness of the deposited coatings before and after submersion in the deionised water bath. These measurements were carried out using a Wyko NT1100 optical profilometer operating in vertical scanning interferometry (VSI) mode. The roughness values are quoted as R_q and R_a values, the former is a measure of mean square roughness, whilst R_a is an arithmetic average roughness of the surfaces. The difference between R_a and R_q is an indication of the homogeneity of surface morphology [12].

Fourier transform infrared spectroscopy (FTIR) measurements were obtained using a Bruker Vertex-70 system with a liquid nitrogen cooled MCT detector and a KBr beam splitter. Spectra were collected in the range of 400-4400 cm^{-1} using a spectral resolution of $4cm^{-1}$ and an overlay of 64 scans per sample cycle.

X-ray photoelectron spectroscopy (XPS) analysis of the samples was carried out in VG Microlab 310-F electron spectrometer at base pressures, in the preparation and analysis chambers, of 2 × 10–8 and 1 × 10–8 Pa, respectively. The photoelectrons were exited with an x-ray source using MgKα ($h\nu$ = 1253.6 eV) and the pass energy of the analyser was 20 eV yielding a resolution of 1.1 eV. The C1s, N1s, O1s, Cl2p & Si2p peaks were recorded along with 50–1000 eV survey scans. The intensities of the peaks were determined as the integrated peak areas assuming the background to be linear.

In order to ascertain the water stability of the coatings deionised water immersion studies were carried out using a Clifton thermal bath (Nickel-Electro Ltd., U.K.) for 180 minutes at 37°C. The samples were then air dried for 5 days and then the properties of the ppAAC coating were reassessed. This involved the use of spectroscopic ellipsometry to measure change in coating thickness, water contact angle measurements, XPS and FTIR to measure changes in chemical functionality.

2.3 Protein Adhesion Studies

Protein adsorption measurements were taken approximately 2 weeks after coating deposition. These studies were carried out with Bovine Serum Albumin (BSA), Immunoglobulin G (IgG) and Fibrinogen (Fg) proteins. Their adsorption was monitored using the Wollam M2000 variable angle spectroscopic ellipsometer which employed a FLS 300 75W Xeon arc lamp operating at an incident angle of 70°, within wavelength limits of 270-1700 nm. Dynamic recording of protein adsorption was carried out through the use of a specially designed LiquidCell™ (TLC-100-02.04 from J.A. Wollam Inc.). This is a specially designed 5 ml cell that allows light from the Xeon source to pass through the liquid cell as protein solution is pumped through the cell, over the sample. The adhesion of protein causes a change in the polarity of the light as it is reflected off the sample surface. These spectroscopic results were analysed using the CompleteEase™ software, supplied with the ellipsometer. Silicon wafers, both coated and uncoated, were exposed to protein solutions. Creating a seal between the liquid cell and the surface of the samples did this. These samples were taped into position using scotch tape to allow the mounting of the cell onto a dedicated ellipsometry stage. A piezoelectric micro-pump (ThinXXS), operating at 10Hz (a flow rate of 2 $ml.min^{-1}$) was used to pump protein solution through an inlet filter (Acrosdisc Supor, Pore size 5 μm) before circulation through the liquid cell. As the protein is suspended in a solution of phosphate buffer solution (PBS), PBS (pH 7.4) was allowed to flow through the cell for 10 minutes in order to establish a baseline signal. PBS containing BSA protein (10 $mg.ml^{-1}$) was then

introduced into the liquid cell. Once the baseline had been set by the PBS solution, the introduction of BSA into the system would, on adhesion to the sample surface, cause a change in optical parameters being monitored by the ellipsometer. In particular there is a change of phase, delta (Δ), and in amplitude, psi (Ψ), from the light being reflected from the samples surface. This was monitored for 40 minutes after the protein solution had been introduced, allowing for a steady state delta reading to be obtained from the ellipsometer. The ellipsometer gathered data from spectral wavelengths of between 300-1100 nm. Data from other wavelengths was omitted as protein adsorption affects the UV region while water causes noise in the IR region. The CompleteEase™ software package used the Cauchy model [27] interoperate the delta change optical parameters observed during the samples exposure to protein solution relate these changes to thickness change at the surface of the sample [28]. After a steady state had been reached in the delta optical measurement PBS was pumped through the system followed by deionised water for a further 10 minutes. This flushed the cell of residual protein. SDS solution flushing of the apparatus completed the cleaning of the liquid cell.

3.0 Results and Discussion

3.1 Preliminary Study

In a preliminary study the effect of precursor flow rate on the thickness and roughness of the AAc coatings deposited using both the air and helium atmospheric plasma systems was investigated. In the case of the PlasmaStream system the flow rate of the AAc precursor was investigated at 5, 10, 20 and 50 μl.min^{-1}, while the He flow was maintained at 6 ml.min^{-1} and that of the N_2 at 60 ml.min^{-1}, the input power was maintained at 90% system power (equivalent to approximately 5.6 kV_{rms} applied voltage). The jet traversed the substrates at a rate of 20 mm/s while the jet orifice to substrate distance was maintained at 2.5 mm.

The ppAAc coatings deposited using the PlasmaTreat system used the same AAc precursor flow rates. In this case however the AAc monomers were passed through a pre-heated heating chamber (55°C), using 2 l.min^{-1} of nitrogen as a carrier gas. The plasma was operated using dry air (delivered at 50 l.min^{-1}), with pulse peak voltages of approximately 5 kV. The plasma source to substrate distance was set to 2 cm, while the plasma traversed the sample at 250 mm.s^{-1}. The coating thickness and roughness (Ra) of these two groups of coatings are given in Figure 3. The same number of passes was used for both systems (5 treatments), however the jet speed of the PlasmaTreat sample is higher than that of the PlasmaStream system. While the coatings are thus not directly comparable, with the processing speed of the PlasmaTreat jet being 12.5 times faster than that of the PlasmaStream system, the corresponding layer thickness at a flow rate of 20 μl.min^{-1} is 114 and 22 respectively. This would indicate a faster coating deposition rate using the PlasmaTreat system (for the same treatment time). Based on the Ra values the PlasmaTreat coating is also significantly smoother than that obtained using the PlasmaStream system.

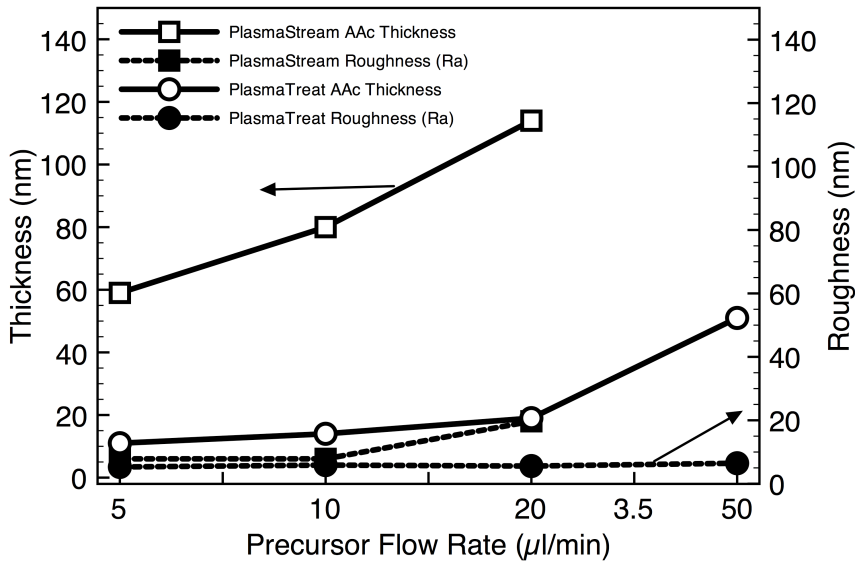

Figure 3: Coating thickness and roughness changes as a result of different precursor AAc flow rates for PlasmaStream and PlasmaTreat systems. Note that while 5 passes of the jet were used for the coating deposition experiments the PlasmaStream jet moved at a process speed of *20 mm.s^{-1} while the PlasmaTreat jet speed was 250 mm.s^{-1}*

Based on these initial studies, the optimised deposition conditions used to compare the two jet systems were as follows: in the case of the PlasmaStream deposition studies, the flow rate of the precursor was set to 5 μl.min^{-1} for 5 passes over the silicon wafer substrate at a gap-height of 2.5 mm. For the PlasmaTreat depositions, AAc was flow rates were set to 5 μl.min^{-1} while the heating coil heated the acid to 55˚C before being delivered to the plasma nozzle, the number of plasma passes over the samples was set to 10.

3.2 Coating Comparison Study

Table 1 summarises the results of the characterisation study of the plasma-polymerised acrylic acid coatings deposited using the two plasma jet systems, both before and after immersion in deionised water. The coatings deposited using the PlasmaStream system, exhibited similar contact angles to the uncoated wafer at 26º. After these measurements were taken it could be seen that the deionised water had dissolved the ppAAC coating where it had come into contact with the sample. After water immersion the coating contact angles increased to 66º indicating a significantly increase in the coatings organic character. Similar changes in WCA for ppAA, after water immersion, have previously been observed and have been ascribed to the loss of COOH functionalities in the coating [29]. The water contact angle of ppAAc coatings deposited using the air plasma system are significantly higher than those deposited using the PlasmaStream system at 52˚. This may indicate a higher level of coating cross-linking and thus greater retention of the functional chemistry of the monomer.

After the water immersion study the WCA of the ppAAc coatings increased by 10˚ indicating that some of the COOH functionality may have been lost during the immersion.

The PlasmaStream's ppAAc coatings exhibited a much higher polar component of surface energy than that deposited using the PlasmaTreat system, which contributes significantly to its hydrophilic properties.

Measurement	ppAAc PlasmaStream	ppAAc PlasmaStream post-immersion	ppAAc PlasmaTreat	ppAAc PlasmaTreat post-immersion
Water contact angle (°)	26 ± 3	66 ± 3	52 ± 1	62 ± 2
Surface Energy (mN/m)	59 ± 3	40 ± 2	50 ± 2	42 ± 2
Dispersive	21 ± 1	27 ± 2	33 ± 1	29 ± 1
Polar	38 ± 3	13 ± 1	17 ± 1	13 ± 1
Roughness (R_a) (nm)	11 ± 4	3 ± 1	5 ± 1	7 ± 1
Roughness (R_q) (nm)	27 ± 5	4 ± 2	7 ± 2	11 ± 2
Thickness (nm)	59 ± 6	4 ± 1	18 ± 2	18 ± 2

Table I: Contact angle, surface energy and roughness data for the ppAAc coatings deposited using both the PlasmaStream and PlasmaTreat systems. The influence of the water immersion studies on the coating properties is also included.

Post-water immersion the roughness (R_a and R_q) of the PlasmaStream deposited coatings exhibit a significant decrease in surface roughness; probably due to a significant level of coating dissolution in the water. In contrast a small increase in the roughness values is observed for the air plasma deposited coatings possibly due to low levels of coating dissolution (but not delamination). The thickness of the optimised PlasmaStream deposited coating was approx. 59 nm thick. This is equivalent to a deposition rate of approx. 12 nm of for each pass of the jet mounted on the CNC (5 passes travelling at 20 $mm.sec^{-1}$). The thickness for the optimised PlasmaTreat systems coating was approx. 18 nm, which equated to approximately 2 nm of film growth per pass of the jet mounted on the CNC (10 passes travelling at 250 $mm.sec^{-1}$).

The infra-red spectra of the AAc monomer and ppAAc coatings deposited using the He and air atmospheric plasma systems are given in Figure 4. This figure also includes changes in the coating FTIR spectra after water immersion. It is clear that the polymerisation process for the two coating deposition techniques causes change to the monomers functionality. The peak observed in the monomer's spectrum around 1440 cm^{-1}, representing C-H, O-H and CH_2 bending and becomes much less intense for the coatings produced, a small peak is however

still present for the PlasmaTreat deposited ppAAc spectra. Similarly the C-O bending peaks at 1234-1167 cm^{-1} also undergo a loss of intensity. The peaks near 1727 cm^{-1} and 1715 cm^{-1}, represent the carbonyl C=O stretching band, are clearly visible in the monomer and on all the PlasmaStream coating spectra [30]. The peak at 1715 cm^{-1} is also present on the PlasmaTreat ppAAc coating however, the peak at 1727 cm^{-1} is absent. The absence of this C=O at 1727 cm^{-1} peak has previously been reported for low pressured deposited plasma polymerised ppAAc coatings [29]. This may explain the difference in WCA between the two ppAAc coatings and my go some way to explaining this coatings stability in water. Both of the PlasmaStream deposited coatings show similar spectra prior to immersion in deionised water. After immersion the PlasmaStream ppAAc coatings exhibit only weak peaks associated with C=O functionality, again indicting a lack of water stability. In the case of the PlasmaTreat deposited coating the peak at 1715 cm^{-1} remains relatively intense after the water immersion study indicating relatively good coating stability. The broad band observed in the AAc monomer's spectrum, at around 2900-3300 cm^{-1}, can also be seen in the PlasmaStream's (prewashing) and the PlasmaTreats's spectra (pre & post-washing). This band represents C-H and O-H symmetric stretching [19]. This band is missing from the PlasmaStream spectra post-washing and is further evidence that this film dissolved in the water.

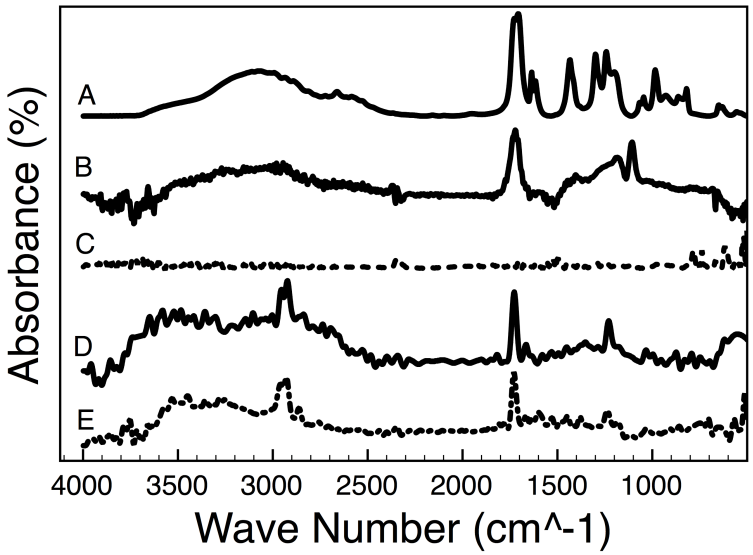

Figure 4: FTIR spectra of the AAc monomer (A), PlasmaStream deposited ppAAc (B) and post-immersion PlasmaStream deposited coating (C). The PlasmaTreat deposited ppAAc (D) and post-immersion (E)

The increased stability of the PlasmaTreat deposited ppAAc coatings, relative to the coatings deposited using the PlasmaStream equivalent, can be explained based on previous studies involving low pressure plasma deposition studies, as being due to an increased level of cross-linking of the polymer film [29]. The PlasmaTreat deposited coatings were found to be stable in air based on a comparative FTIR spectra study carried out both immediately after deposition and again after a 6-month period during which the coating was stored in air. The difference in cross-linking is related to the applied powers of the two deposition systems. The PlasmaStream uses a helium/nitrogen atmospheric plasma, while the PlasmaTreat system uses compressed air. Plasma diagnostic studies of these two sources have previously been reported in detail [23, 24]. Of particular relevance to this study are the optical emission spectroscopy (OES) and thermal imaging analysis of plasmas generated by both systems. OES analysis indicates that the rotational temperature of nitrogen molecules, in a plasma generated by the helium based PlasmaStream system, reached temperatures of approx. 400 K, while the air plasma, generated by the PlasmaTreat system, saw these temperatures reach over 1900 K. The translational energy distribution of a gas is closely coupled to the population distribution among molecular nitrogen sublevels. It is therefore generally considered that the rotational

temperature is similar to the kinetic gas temperature [31], this view however has recently been challenged by the use of fibre-optic based devices to obtain temperature measurement [32]. Thermal imaging examinations have also shown a large difference in the temperatures generated by the systems [23, 24]. The maximum gas temperature observed on the PlasmaStream system was 374 K, while the PlasmaTreat system had a gas temperature of approximately 550 K, 15 mm downstream of the plasma nozzle. The increased kinetic gas temperature of the PlasmaTreat system, coupled with the higher thermal emissions from the air plasma, indicate that more energy was imparted to the AAc monomer by the PlasmaTreat system. This increased energy may have lead to more cross-linking of the ppAAc polymer and allowed the formation of water stable film.

XPS analysis was carried out on PlasmaTreat ppAAc deposited coatings (Figure 5). It was used to further investigate whether the water immersion (180 mins at 37° C) of the sample effected the chemical composition of the ppAAc. The theoretical percentage of the functional groups, as a percentage of total carbon is displayed in Table 2. Based on the procedure set out by Beck *et al*. the percentage carboxylate retained in the ppAAc, relative to the AAc monomer, is 68 % [7]. C-O bonds are formed during the plasma deposition process, evidence of the polymerisation processes undergone by the AAc monomer. The percentage of carboxylate in the coating is 22.8 %, which is lower than the 33.3 % theoretical percentage. However, the lower level of C-O bonds (13.5 %) and the lack of excess C-C/C-H bonds (63.7 %), would indicate that a large percentage of the carboxylates are present as carboxylic acid, reained from the AAc monomer. This conclusion is supported by the retention of some of the O-H peak, at 1440 cm^{-1}, in the coatings FTIR spectra (Figure 4). Immersing the sample in deionised water decreases the amount of retained carboxylate to 45 % of the theoretical amount present in the AAc monomer. This represents 14.9 % of the overall coating functionality and is similar to the values reported for water stable ppAAc coatings deposited at low pressure [14]. The XPS analysis also indicated that trace (<1%) concentrations of

tungsten and copper were present in the ppAAc coating, probably due to small amounts of the metal being removed from the electrode or nozzle in the blown arc PlasmaTreat source, during the coating deposition process.

	CH/CC (% of total carbon)	C-O (% of total carbon)	COOR (% of total carbon)	% Retention COOR from AAc
Binding Energies (eV)	285	286.6	289.2	
ppAAc	63.7 %	13.5 %	22.8 %	68.4 %
ppAAc Post-immersion	68 %	17.1 %	14.9 %	44.7 %
Theoretical value for AAc	66.67%	0 %	33.33 %	

Table II: XPS analysis of PlasmaTreat deposited ppAAc coatings obtained both before and after water immersion. Binding energies are shown for moieties observed in the coating as well as the percentage of CC/CH, C-O and COOR, as a percentage of the total theoretical carbon content, of the AAc monomer. The percentage of COOR retained as a percentage of theoretical COOR of the AAc monomer is also displayed.

Having established using both FTIR and XPS examination that ppAAc coatings deposited using the Air system exhibited relatively good water stability, these were selected for the room temperature aqueous based protein adhesion studies. The initial study carried out using the spectroscopic ellipsometer involved monitoring changes in coating thickness with time in the flowing PBS solution. A gradual change in the optical parameter delta from its baseline signal was observed over a period of 60 minutes. This delta change is directly related to a change in layer thickness [27]. By fitting a Cauchy model to the change in ellipsometry data, a change in film thickness was observed as illustrated in Figure 6 [28]. A film thickness reduction of approximately 0.2 nm is observed over this 60-minute period for the 18 nm thick ppAAc coating.

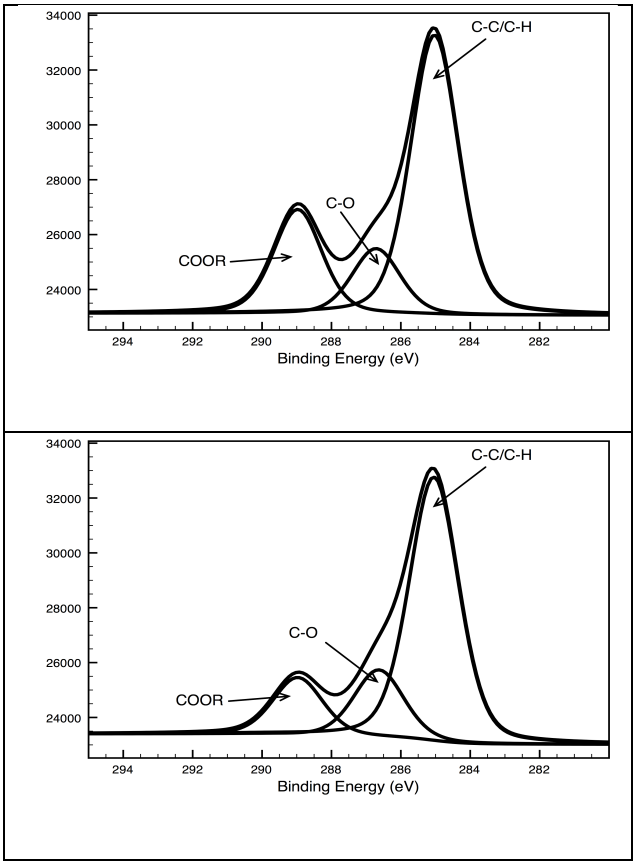

Figure 5: XPS spectra of the C1s peaks of the PlasmaTreat deposited ppAAc (top) and post-water immersion (bottom)

3.3 Protein Adhesion

The adhesion of the BSA, IgG and Fg proteins onto PlasmeTreat deposited ppAAc coating was investigated using the spectroscopic ellipsometry technique. The layer thickness of the proteins deposited in the flow cell system was determined in a manner similar to that used to investigate coating stability. A phosphate buffer solution was circulated over the coated and uncoated silicon wafers for approximately 10 minutes prior to the introduction of each protein solution. Introduction of the protein solution onto the uncoated silicon resulted in the adhesion of a protein layer for all three proteins. In the case of BSA, an 8° increase in the optical parameter delta, relative to it's baseline signal, was observed. This delta change is directly related to a change in BSA layer thickness. No further change in delta was observed for the test period of 30 minutes, while the BSA solution was circulating over the wafer. By fitting a Cauchy model to the change in ellipsometry data, the BSA layer thickness on the

uncoated silicon wafer was calculated as approximately 2 nm (Figure 7) [33].This is in agreement with BSA protein layer thickness reported previously on SiO2 substrates, where a BSA protein layer of 2.3 nm was reported for SiO2 substrates [34]. Similarly Fg and IgG layer thickness plateau at an average of 4 nm (Figure 8) and 2 nm (Figure 9) respectfully. The fibrinogen layer thickness result of 4 nm is within the range of 2 to 10 nm thickness previously reported for the adhesion of this protein onto silicon wafer substrates [35, 36].

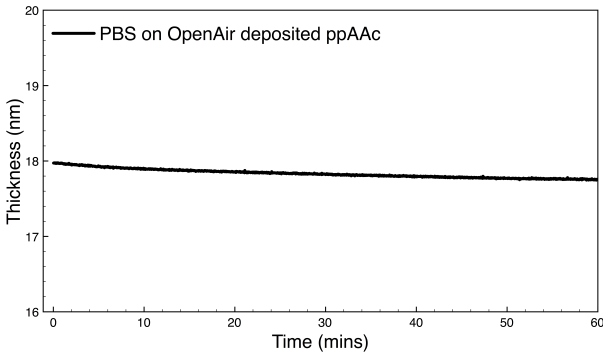

Figure 6: Dynamic coating thickness change measured using ellipsometry on exposure of the ppAAc coating to the phosphate buffer solution (PBS)

Having carried out the baseline studies with the three proteins on silicon wafer substrates the next step is to investigate the effect of the ppAAc coatings. The interaction of BSA protein solution with ppAAc is illustrated in Figure 7. Over the 10-minute period prior to the addition of the protein solution there is a no change in the surface layer thickness. On the introduction of the protein solution to the liquid cell a thickness increase of approximately 4 nm is seen. As the BSA protein has dimensions of 4x4x14 nm [37], this result would indicate that a side on, specifically bound protein layer initially forms on the ppAAc surface. Protein layer thickness was then observed to increase at a much slower rate. The first of these two phases in protein adhesion is the direct attachment of protein molecules onto the ppAAc surface, while the second slower phase is most likely due to protein conformational changes. BSA protein, and proteins in general, have been shown to bind to hydrophobic surfaces in thicker layers than hydrophobic surfaces [38]. On hydrophobic surfaces (such as the uncoated silicon wafer) the

main adsorption driving forces are hydrogen bonding and electrostatic interactions, while hydrophobic interactions become dominant on the more hydrophobic surface [39]. The increase in hydrophobicity between the bare silicon wafer and the ppAAc coating may also be the cause of this increased protein layer thickness.

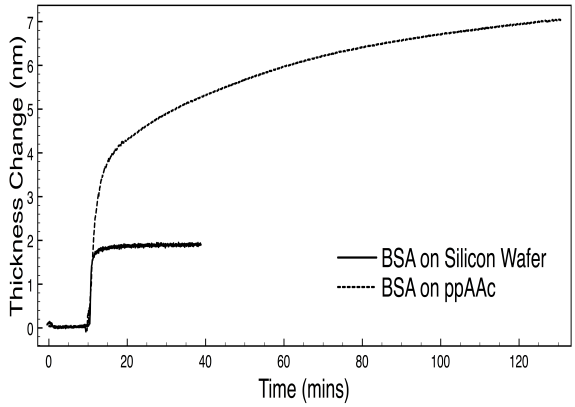

Figure 7: Change in layer thickness for BSA exposed to uncoated (solid) and ppAAc coated (dashed) silicon wafer surfaces. The protein was introduced into the buffer solution at the 10 minute time point.

Figure 8 presents the results of the Fibrinogen protein adhesion study. When the Fg is added to the buffer solution flowing over the bare silicon wafer a step change in thickness. It was observed that a protein layer thickness of 5 nm formed on the ppAAc coating. This is slightly thicker than the layer that adhered to the uncoated silicon. The rate of protein layer adhesion is not as rapid with the ppAAc film when compared with the silicon wafer substrate. It takes the protein almost 1 hour to establish a steady state thickness on the ppAAc, while it is almost instantaneous on the bare wafer. During this time the adsorption thickness on the ppAAc undulates, this has been previously reported in Fg interactions with carbon/hydrogen based thin films [40]. The Fg molecule dimensions of 6x6x45 nm so the final steady state thickness of 5 nm would indicate that a side on orientated, partially denatured, protein layer had adhered to the ppAAc.

As illustrated in Figure 9, the addition of IgG causes a similar thickness change, of 7 nm, on the ppAAc coatings to that of the of the BSA molecule. This was higher than was observed

for the bare silicon wafer (2 nm). The adhesion of IgG protein has two distinct phases. The first 20 minutes after the protein is added to the solution sees a relatively rapid increase of protein thickness. After 20 minutes the thickness reaches 4 nm. This correlates with the proteins 4 nm thick protein and would indicate that the protein initially adheres in a side on, monolayer, orientation. 20 minutes after the introduction of the protein the rate of adhesion slows. This change in adhesion rate may be as a result of non-specific interactions between the first, specifically bound monolayer of IgG, molecules and randomly adsorbed IgG proteins from the solution. This has been previously reported on IgG adhesion on protein-A terminated surfaces [41].

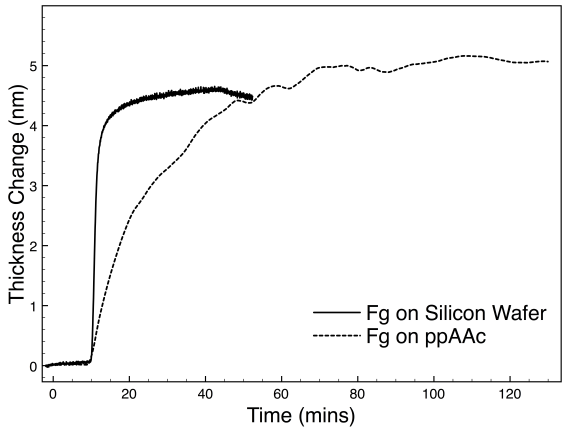

Figure 8: Uncoated (solid) and ppAAc coated (dashed) silicon wafer on exposure to Fg protein solution

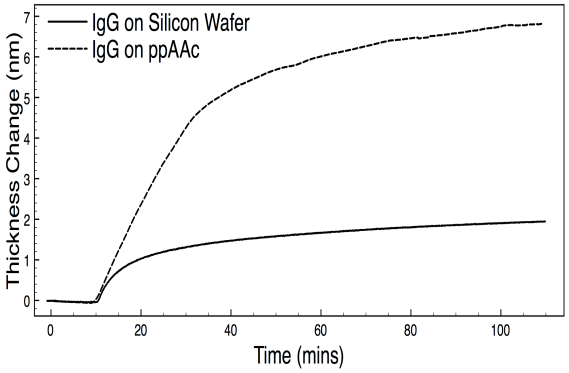

Figure 9: Uncoated (solid) and ppAAc coated (dashed) silicon wafer exposure to IgG protein solution

4.0 Conclusions

This study reports that water-stable polymerised acrylic acid coatings have been formed using the PlasmaTreat atmospheric plasma deposition system. XPS analysis indicated that these

coatings retained a high level of carboxylates in the polymerised film, a large percentage of which was made up of carboxylic moieties from the AAc monomer. Water stable coatings were not achieved for the ppAAc coatings deposited using the helium based PlasmaStream however. FTIR analysis showed ppAAc deposited by the PlasmaStream system were unstable in aqueous solution as only trace amounts remained after water immersion. Ellipsometry measurements demonstrated only a 0.2 nm reduction in the thickness of an 18 nm thick PlasmaTreat deposited ppAAc coating, when immersed in an aqueous buffer solution for one hour. The increased stability of the PlasmaTreat coatings, relative to those deposited using the PlasmaStream system is likely to be due to an increase in the cross-linking of the polymer film, which is related to the relative plasma intensities of the He and air plasma jet deposition systems.

Protein adhesion studies were carried out, using BSA, Fg and IgG protein solutions, on the water stable ppAAc films. The adhesion of these proteins under flow conditions was monitored using spectroscopic ellipsometry. It was observed that all three proteins studied, showed an increase in layer thickness, relative to the bare silicon wafer substrate. BSA, Fg and IgG protein adhesion to the ppAAc layer appeared to take place in two stages: firstly a rapid rate of adhesion and increase of thickness was observed, this was followed by a longer period of protein reorientation, which resulted in a slow increase in protein layer thickness values. This behaviour was in contrast to the silicon wafer substrates, which initially yielded a rapid rate of protein adhesion once they was introduced into the buffer solution and then a relatively constant level of adhesion. For all three proteins higher levels of adhesion are observed on the ppAAc films compared with that on the wafer substrate as shown in the following table -

Protein layer thickness (nm)

	BSA	Fg	IgG
Silicon wafer	2	4	2

ppAAc 7 5 7

The increased thickness was most likely due to the combined affects of the increased hydrophobicity of the surface and the different orientation of the protein molecules on the silicon wafer and ppAAc surfaces.

Acknowledgements

This work is supported by Science Foundation Ireland Grant 08/SRCI1411

References

[1] Nakanishi K, Sakiyama T, Imamura K. On the adsorption of proteins on solid surfaces, a common but very complicated phenomenon. Journal of Bioscience and Bioengineering 2001;91:233.

[2] Hlady V, Buijs J. Protein adsorption on solid surfaces. Current Opinion in Biotechnology 1996;7:72.

[3] Anderson J. Biological responses to materials. . Annu. Rev. Mater. Res 2001:81.

[4] Chen H, Yuan L, Song W, Wu Z, Li D. Biocompatible polymer materials: Role of protein-surface interactions. Progress in Polymer Science 2008;33:1059.

[5] Moradi O, Modarress H, Noroozi M. Experimental study of albumin and lysozyme adsorption onto acrylic acid (AA) and 2-hydroxyethyl methacrylate (HEMA) surfaces. Journal of Colloid and Interface Science 2004;271:16.

[6] Johansson C, Gernandt J, Bradley M, Vincent B, Hansson P. Interaction between lysozyme and colloidal poly(NIPAM-co-acrylic acid) microgels. Journal of Colloid and Interface Science 2010;347:241.

[7] Beck AJ, Short RD, Matthews A. Deposition of functional coatings from acrylic acid and octamethylcyclotetrasiloxane onto steel using an atmospheric pressure dielectric barrier discharge. Surface and Coatings Technology 2008;203:822.

[8] Lee NY, Lim JR, Kim YS. Selective patterning and immobilization of biomolecules within precisely-defined micro-reservoirs. Biosensors and Bioelectronics 2006;21:2188.

[9] Konig U, Nitschke M, Menning A, Eberth G, Pilz M, Arnhold C, Simon F, Adam G, Werner C. Durable surface modification of poly(tetrafluoroethylene) by low pressure H2O plasma treatment followed by acrylic acid graft polymerization. Colloids and Surfaces B: Biointerfaces 2002;24:63.

[10] Albaugh J, O'Sullivan C, O'Neill L. Controlling deposition rates in an atmospheric pressure plasma system. Surf. Coat. Technol 2008;203:844.

[11] GonÁalves G, Marques PAAP, Trindade T, Neto CP, Gandini A. Superhydrophobic cellulose nanocomposites. Journal of Colloid and Interface Science 2008;324:42.

[12] Stallard C, McDonnell K, Donegan M, Dowling D. Evaluation of spectroscopic ellipsometry for the measurement of BSA protein adhesion on atmospheric plasma modified surfaces. European Conference for Nano Films. Liege, Belgium, 2010.

[13] Ko T-M, Lin J-C, Cooper SL. Surface Characterization and Platelet Adhesion Studies of Plasma-Carboxylated Polyethylene. Journal of Colloid and Interface Science 1993;156:207.

[14] Lopez LC, Gristina R, Ceccone G, Rossi F, Favia P, d'Agostino R. Immobilization of RGD peptides on stable plasma-deposited acrylic acid coatings for biomedical devices. Surface and Coatings Technology 2005;200:1000.

[15] Daw R, Candan S, Beck AJ, Devlin AJ, Brook IM, MacNeil S, Dawson RA, Short RD. Plasma copolymer surfaces of acrylic acid/1,7 octadiene: Surface characterisation and the attachment of ROS 17/2.8 osteoblast-like cells. Biomaterials 1998;19:1717.

[16] Detomaso L, Gristina R, Senesi GS, d'Agostino R, Favia P. Stable plasma-deposited acrylic acid surfaces for cell culture applications. Biomaterials 2005;26:3831.

[17] France R, RD Short, RA Dawson, Macneil. Attachment of human keratinocytes to plasma co-polymers of acrylic

acid/octa-1,7-diene and allyl amine/octa-1,7-diene. Journal of Materials Chemistry 1998;8:37.

[18] Lee S-D, Hsiue G-H, Chang PC-T, Kao C-Y. Plasma-induced grafted polymerization of acrylic acid and subsequent grafting of collagen onto polymer film as biomaterials. Biomaterials 1996;17:1599.

[19] Sciarratta V, Vohrer U, Hegemann D, M¸ller M, Oehr C. Plasma functionalization of polypropylene with acrylic acid. Surface and Coatings Technology 2003;174-175:805.

[20] Dhayal M, Cho S-I. Leukemia cells interaction with plasma-polymerized acrylic acid coatings. Vacuum 2006;80:636.

[21] Topala I, Dumitrascu N, Popa G. Properties of the acrylic acid polymers obtained by atmospheric pressure plasma polymerization. Nuclear Instruments and Methods in Physics Research Section B: Beam Interactions with Materials and Atoms 2009;267:442.

[22] O'Neill L, Shephard N, Leadley S. Plasma Polymerised Primers- Improved Adhesion Through Polymer Coatings. 50th Annual Technical Conference Proceedings of the Society of Vacuum Coaters, 2007.

[23] Nwankire C, Law V, Nindrayog A, Twomey B, Niemi K, Milosavljević V, Graham W, Dowling D. Electrical, Thermal and Optical Diagnostics of an Atmospheric Plasma Jet System. Plasma Chemistry and Plasma Processing 2010;30:537.

[24] Dowling DP, O'Neill FT, Langlais SJ, Law VJ. Influence of dc Pulsed Atmospheric Pressure Plasma Jet Processing Conditions on Polymer Activation. Plasma Processes and Polymers 2011;8:718.

[25] Owens D, Wendt R. Estimation of the Surface Free Energy of Polymers. Journal of applied polymer science. 1969;13:1741.

[26] Storm G, Fredirksson M, Stenius P. Contact Angles, Work of Adhesion, and Interfacial Tensions at a Dissolving Hydrocarbon Surface. J. Colloid. Interface Sci. 1986;119(2).

[27] Tompkins, MaGahan. Spectroscopic Ellipsometry and Reflectometry. New York: John Wiley & Sons, 1999.

[28] Arwin H. Handbook of Ellipsometry. Heidelberg: Springer-Verlag GmbH & Co. KG, 2005.

[29] Jafari R, Tatoulian M, Morscheidt W, Arefi-Khonsari F. Stable plasma polymerized acrylic acid coating deposited on polyethylene (PE) films in a low frequency discharge (70†kHz). Reactive and Functional Polymers 2006;66:1757.

[30] Sciarratta V, Vohrer U, Hegemann D, M¸ller M, Oehr C. Plasma functionalization of polypropylene with acrylic acid. Surface and Coatings Technology;174-175:805.

[31] Laux CO, Spence TG, Kruger CH, Zare RN. Optical diagnostics of atmospheric pressure air plasmas. Plasma Sources Science and Technology 2003;12:125.

[32] Wertheimer MR, Ahlawat M, Saoudi B, Kashyap R. Accurate in-situ gas temperature measurements in dielectric barrier discharges at atmospheric pressure. Applied Physics Letters 2012;100:201112.

[33] Arwin H. Handbook of Ellipsometry. Ellipsometry in Life Sciences. Heidelberg: Springer-Verlag GmbH & Co. KG, 2005.

[34] Seitz RB, Geiger aR. Protein adsorption on solid–liquid interfaces monitored by laser-ellipsometry. Applied Surface Science 2005;252 154–15.

[35] Joshi O, Lee HJ, McGuire J, Finneran P, and Bird KE. Protein concentration and adsorption time effects on fibrinogen adsorption at heparinized silica interfaces. Colloids and Surfaces B: Biointerfaces 2006;50:26.

[36] Choukourov AGA, Saito N. and Takai O. SPM analysis of fibrinogen adsorption on solid surfaces. Surface Science 2007;601:3948.

[37] McClellan SJ, Franses EI. Adsorption of bovine serum albumin at solid/aqueous interfaces. Colloids and Surfaces A: Physicochemical and Engineering Aspects 2005;260:265.

[38] Malmsten M. Formation of Adsorbed Protein Layers. Journal of Colloid and Interface Science 1998;207:186.

[39] Ying P, Jin G, Tao Z. Competitive adsorption of collagen and bovine serum albumin,Äîeffect of the surface wettability. Colloids and Surfaces B: Biointerfaces 2004;33:259.

[40] Lousinian S, Logothetidis S. In-situ and real-time protein adsorption study by Spectroscopic Ellipsometry. Thin Solid Films 2008;516:8002.

[41] Zengin A, Caykara T. Immobilization of immunoglobulin G in a highly oriented manner on a protein-A terminated multilayer system. Applied Surface Science 2011;257:2111.

List of Tables

Table I: Contact angle, surface energy and roughness data for the ppAAc coatings deposited using both the PlasmaStream and PlasmaTreat systems. The influence of the water immersion studies on the coating properties is also included.

Measurement	ppAAc PlasmaStream	ppAAc PlasmaStream post-immersion	ppAAc PlasmaTreat	ppAAc PlasmaTreat post-immersion
Water contact angle (º)	26 ± 3	66 ± 3	52 ± 1	62 ± 2
Surface Energy (mN/m)	59 ± 3	40 ± 2	50 ± 2	42 ± 2
Dispersive	21 ± 1	27 ± 2	33 ± 1	29 ± 1
Polar	38 ± 3	13 ± 1	17 ± 1	13 ± 1
Roughness (R_a) (nm)	11 ± 4	3 ± 1	5 ± 1	7 ± 1
Roughness (R_q) (nm)	27 ± 5	4 ± 2	7 ± 2	11 ± 2

Table II: XPS analysis of PlasmaTreat deposited ppAAc coatings obtained both before and after water immersion. Binding energies are shown for moieties observed in the coating as well as the percentage of CC/CH, C-O and COOR, as a percentage of the total theoretical carbon content, of the AAc monomer. The percentage of COOR retained as a percentage of theoretical COOR of the AAc monomer is also displayed.

	CH/CC (% of total carbon)	C-O (% of total carbon)	COOR (% of total carbon)	% Retention COOR from AAc
Binding Energies (eV)	285	286.6	289.2	
ppAAc	63.7 %	13.5 %	22.8 %	68.4 %
ppAAc Post-immersion	68 %	17.1 %	14.9 %	44.7 %
Theoretical value for AAc	66.67%	0 %	33.33 %	

List of Figures

Figures

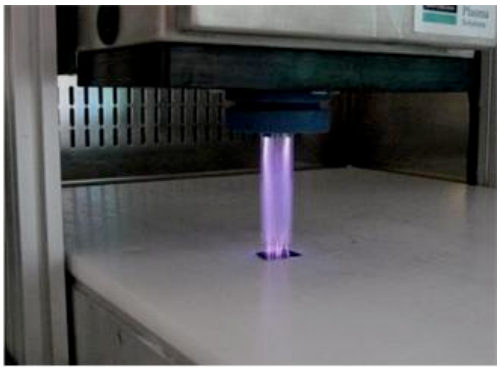

1

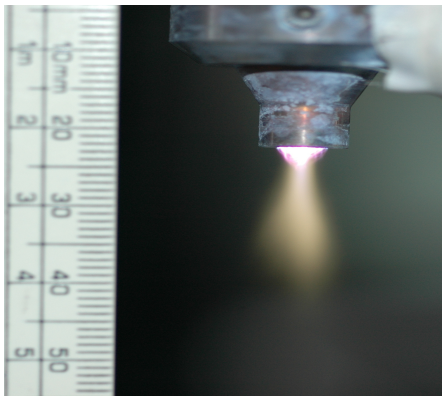

2

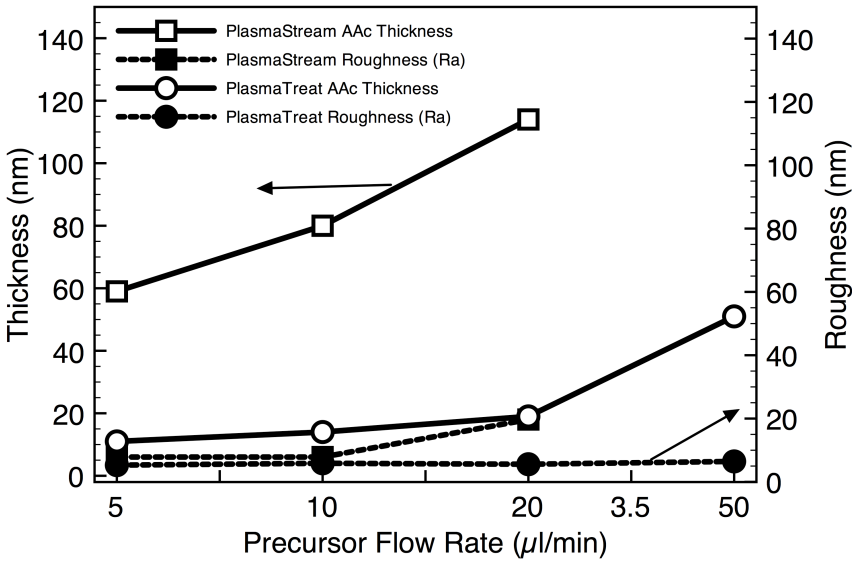
PlasmaStream AAc Thickness
PlasmaStream Roughness (Ra)
PlasmaTreat AAc Thickness
PlasmaTreat Roughness (Ra)
Thickness (nm)
Roughness (nm)
0
20
40
60
80
100
120
140
5
10
20
3.5
50
Precursor Flow Rate (μl/min)

3

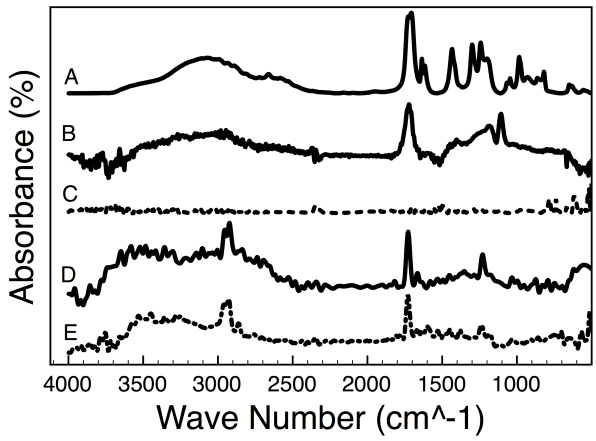
Absorbance (%)
A
B
C
D
E
4000 3500 3000 2500 2000 1500 1000
Wave Number (cm^-1)

4

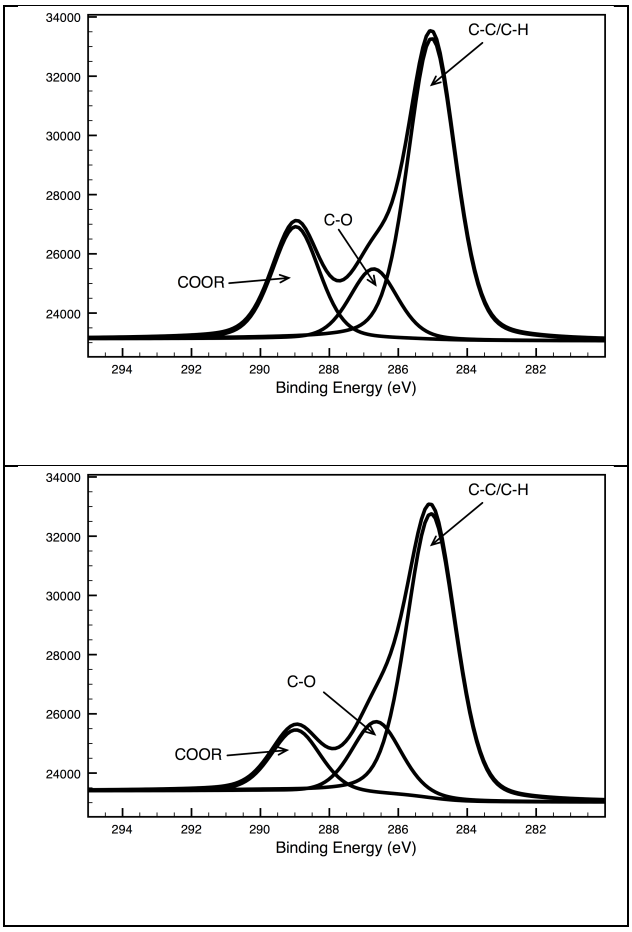
34000
32000
30000
28000
26000
24000
C-C/C-H
C-O
COOR
294 292 290 288 286 284 282
Binding Energy (eV)
34000
32000
30000
28000
26000
24000
C-C/C-H
C-O
COOR
294 292 290 288 286 284 282
Binding Energy (eV)

5

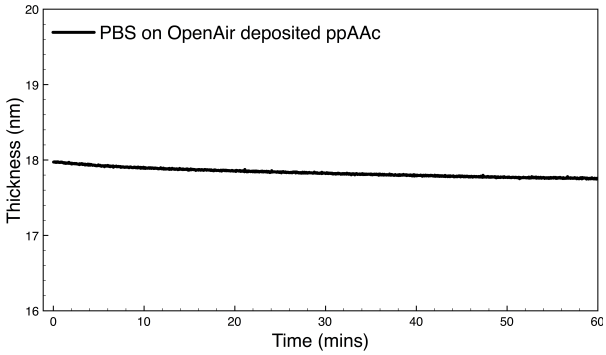
PBS on OpenAir deposited ppAAc
Thickness (nm)
Time (mins)

6

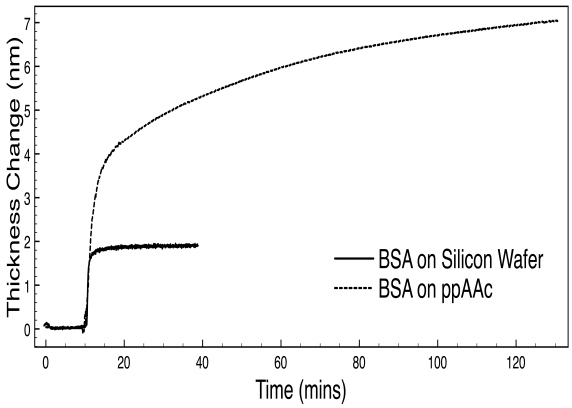
BSA on Silicon Wafer
BSA on ppAAc
Thickness Change (nm)
Time (mins)

7

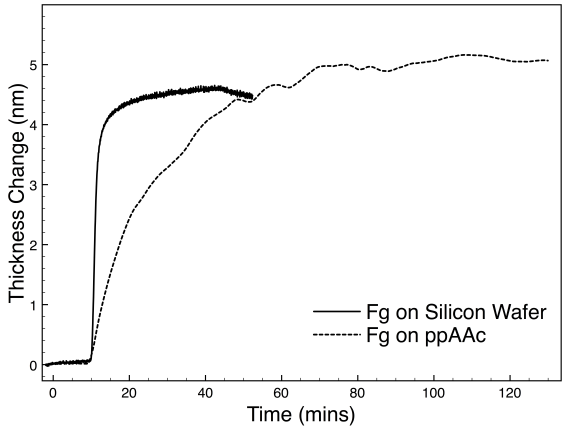
Fg on Silicon Wafer
Fg on ppAAc
Thickness Change (nm)
Time (mins)

8

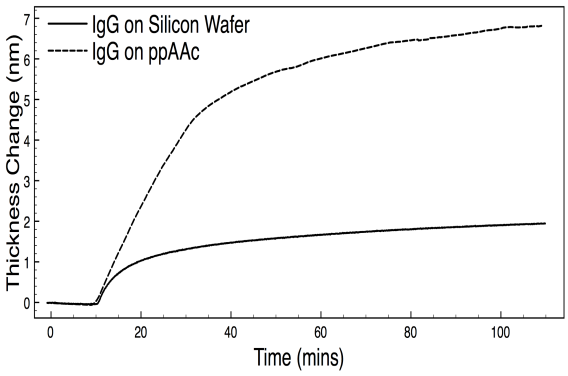
IgG on Silicon Wafer
IgG on ppAAc
Thickness Change (nm)
0
1
2
3
4
5
6
7
0
20
40
60
80
100
Time (mins)